

# **SANDIA REPORT**

SAND2011-7311

Unlimited Release

Printed October 2011

## **Confined Cooperative Self-Assembly and Synthesis of Optically and Electrically Active Nanostructures: Final LDRD Report**

Hongyou Fan, Feng Bai, Anh Ta, Raid E. Haddad, Eric N. Coker, Jianyu Huang, and Mark A. Rodriguez

Prepared by  
Sandia National Laboratories  
Albuquerque, New Mexico 87185

Sandia National Laboratories is a multi-program laboratory managed and operated by Sandia Corporation, a wholly owned subsidiary of Lockheed Martin Corporation, for the U.S. Department of Energy's National Nuclear Security Administration under contract DE-AC04-94AL85000.

Approved for public release; further dissemination unlimited.



**Sandia National Laboratories**

Issued by Sandia National Laboratories, operated for the United States Department of Energy by Sandia Corporation.

**NOTICE:** This report was prepared as an account of work sponsored by an agency of the United States Government. Neither the United States Government, nor any agency thereof, nor any of their employees, nor any of their contractors, subcontractors, or their employees, make any warranty, express or implied, or assume any legal liability or responsibility for the accuracy, completeness, or usefulness of any information, apparatus, product, or process disclosed, or represent that its use would not infringe privately owned rights. Reference herein to any specific commercial product, process, or service by trade name, trademark, manufacturer, or otherwise, does not necessarily constitute or imply its endorsement, recommendation, or favoring by the United States Government, any agency thereof, or any of their contractors or subcontractors. The views and opinions expressed herein do not necessarily state or reflect those of the United States Government, any agency thereof, or any of their contractors.

Printed in the United States of America. This report has been reproduced directly from the best available copy.

Available to DOE and DOE contractors from  
U.S. Department of Energy  
Office of Scientific and Technical Information  
P.O. Box 62  
Oak Ridge, TN 37831

Telephone: (865) 576-8401  
Facsimile: (865) 576-5728  
E-Mail: [reports@adonis.osti.gov](mailto:reports@adonis.osti.gov)  
Online ordering: <http://www.osti.gov/bridge>

Available to the public from  
U.S. Department of Commerce  
National Technical Information Service  
5285 Port Royal Rd.  
Springfield, VA 22161

Telephone: (800) 553-6847  
Facsimile: (703) 605-6900  
E-Mail: [orders@ntis.fedworld.gov](mailto:orders@ntis.fedworld.gov)  
Online order: <http://www.ntis.gov/help/ordermethods.asp?loc=7-4-0#online>



# SANDIA REPORT

SAND2011-7311

Unlimited Release

Printed October 2011

## Confined Cooperative Self-Assembly and Synthesis of Optically and Electrically Active Nanostructures: Final LDRD Report

Hongyou Fan <sup>a,\*</sup>, Feng Bai <sup>b</sup>, Anh Ta <sup>b</sup>, Raid E. Haddad <sup>b</sup>, Eric N. Coker <sup>a</sup>, Jianyu Huang <sup>c</sup>, and Mark A. Rodriguez <sup>d</sup>

<sup>a</sup> Ceramic Processing and Inorganic Materials Department, Sandia National Laboratories, P.O. 5800, Albuquerque, NM 87185-1349

<sup>b</sup> Center for Micro-engineered Materials, Chemical and Nuclear Engineering Department, University of New Mexico, Albuquerque, NM 87131,

<sup>c</sup> Center for Integrated Nanotechnologies, Sandia National Laboratories, Albuquerque, NM 87185

<sup>d</sup> Materials Characterization, Sandia National Laboratories, Albuquerque, NM 87185

### Abstract

In this project, we developed a confined cooperative self-assembly process to synthesize one-dimensional (1D) j-aggregates including nanowires and nanorods with controlled diameters and aspect ratios. The facile and versatile aqueous solution process assimilates photo-active macrocyclic building blocks inside surfactant micelles, forming stable single-crystalline high surface area nanoporous frameworks with well-defined external morphology defined by the building block packing. Characterizations using TEM, SEM, XRD, N<sub>2</sub> and NO sorption isotherms, TGA, UV-vis spectroscopy, and fluorescence imaging and spectroscopy indicate that the j-aggregate nanostructures are monodisperse and may further assemble into hierarchical arrays with multi-modal functional pores. The nanostructures exhibit enhanced and collective optical properties over the individual chromophores. This project was a small footprint research effort which, nonetheless, produced significant progress towards both the stated goal as well as unanticipated research directions.

## **Acknowledgements**

*This work was performed by an interdisciplinary team including Sandia National Laboratories and university of New Mexico Sandia National Laboratories is a multi-program laboratory managed and operated by Sandia Corporation, a wholly owned subsidiary of Lockheed Martin Corporation, for the U.S. Department of Energy's National Nuclear Security Administration under contract DE-AC04-94AL85000.*

## Table of Contents

Acknowledgments.....	4
Executive Summary .....	7
1. Introduction.....	7
2. Results and Discussion .....	8
3. Conclusions.....	17
4. References.....	18
5. Appendix.....	20
6. Distribution .....	27

## List of Figures and Tables

Figure 1. Structure of the self-assembled j-aggregate nanostructures .....	11
Figure 2. Representative SEM images showing controlled size and aspect ratio of 1D nanostructures .....	13
Figure 3. Macrocyclic monomer aggregation at different reaction times. ....	14
Figure 4. Nitrogen isotherms. ....	15
Table 1. Porosity, surface area, and pore size of different ZnTPyP nanostructures.....	15

# **Confined Cooperative Self-Assembly and Synthesis of Optically and Electrically Active Nanostructures: Final LDRD Report**

## **Executive Summary**

The purpose of this LDRD is to develop a confined cooperative self-assembly process to synthesize one-dimensional (1D) organic conjugated nanostructures including nanowires and nanorods. Through surfactant-assisted non-covalent interactions, nanorods and nanowires with controlled dimension and morphology can be prepared using zinc meso-tetra (4-pyridyl) porphyrin (ZnTPyP) as the molecular building block. The 1D nanostructures exhibit unique optical and electrical properties, enhanced over properties of individual monomers due to collective behavior resulting from their assembly. Through kinetic control, our method readily allows for fine-tuning of nanostructure, dimension, and function on multiple length scales. At the molecular level, ZnTPyPs with well-defined size and chemistry possess unique optical and photo-catalytic properties for synthesis of metallic structures. On the nanoscale, controlled assembly of macrocyclic monomers leads formation of ordered nanostructures with precisely defined size, shape, and spatial monomer arrangement so as to facilitate intermolecular mass and energy transfer or delocalization. The capability of exerting rational control over dimension and morphology provides new opportunities for applications in sensing, nanoelectronics, and optics.

## **1. Introduction**

Porous one-dimensional (1D) j-aggregate nanostructures, such as nanowires and nanorods, exhibit enhanced applications in nanoelectronics, sensing, and catalysis due to

their increased surface areas and reduced densities.<sup>1-3</sup> Continuous extensive efforts have been made to develop methods to fabricate 1D porous nanostructures,<sup>1</sup> such as templating methods,<sup>4, 5</sup> hydrothermal synthesis,<sup>6</sup> non-covalent self-assembly,<sup>7, 8</sup> and coordination modulation growth<sup>9</sup>. Molecular self-assembly is one of the powerful methods to fabricate porous hierarchical nanostructures that impart multifunctionality derived from individual starting molecules or molecular building blocks.<sup>3</sup> Pore structures, morphologies, and function can be readily controlled through cooperative self-assembly through specific non-covalent interactions as well as control of shape and size of starting molecules. Harnessing these advantages of molecular self-assembly, we report here a surfactant micelle confined process to develop a cooperative self-assembly in combination with functional macrocyclic building blocks to synthesize highly ordered 1D j-aggregate nanostructures that exhibit enhanced optical activity.

## **2. Results and Discussion**

Macromolecules such as chlorophyll and heme, etc. with well-defined size and chemistry are essential pigments in many biological energy transduction processes in plants, algae, and bacteria, including light harvesting, photo-catalytic synthesis, water splitting, etc.<sup>10-12</sup> Inspired by their utility and function, here we use their relative zinc meso-tetra (4-pyridyl) porphyrin (ZnTPyP) as the molecular building block to synthesize 1D j-aggregates. ZnTPyP has well-defined size (~1.6-nm×1.6-nm×0.5-nm) and surface chemistry; its four peripheral pyridine groups allow coordination to metal ions to form self-assembled single crystalline networks. The first step in our confined self-assembly synthesis is encapsulation of ZnTPyP within the core of surfactant micelles through an interfacially driven aqueous process.<sup>13</sup> ZnTPyP does not dissolve in water due to its hydrophobic nature. It has been shown that the four pyridine groups of ZnTPyP will be

protonated at low pH to form the tetrapyrindinium cation  $\text{ZnTPyPH}_4^{4+}$  that dissolves in the aqueous phase forming a homogeneous solution.<sup>14</sup> To initiate the encapsulation process, the  $\text{ZnTPyPH}_4^{4+}$  acidic aqueous solution is added to a basic aqueous solution of surfactant [ $c_{\text{surfactant}} > \text{critical micelle concentration (cmc)}$ ] under vigorous stirring with a range of volume ratios (see experimental details in Supporting Information).

Acid-base neutralization deprotonates the tetrapyrindinium cations producing hydrophobic ZnTPyPs that are thus encapsulated within the hydrophobic micellar interiors as typically happens with hydrophobic nanoparticles or oil-like species.<sup>13, 15</sup> Further self-assembly driven by intermolecular axial coordination (Zn-N) or non-covalent interactions such as hydrophobic-hydrophobic interactions and aromatic  $\pi$ - $\pi$  stacking between macrocyclic molecules or surfactants initiates nucleation and growth of ZnTPyP j-aggregate nanostructures.

The nanostructures produced have well-defined 1D morphologies, including nanorods and nanowires as illustrated in Figure 1. Figure 1A shows a representative scanning electron microscopy (SEM) image of the ZnTPyP nanorods. The nanorods have hexagonal external profile with narrow size distribution in both length and diameter. The average diameter of the nanorods is 150 nm (standard deviation 10%) and the aspect ratio can be controlled in a range from 2 to 10. The monodispersity of these nanorods allows them to further form ordered hexagonal arrays. Transmission electron microscopy (TEM) characterization (Figure 1B) reveals that these 1D nanostructures show a uniform electron contrast without defects. The cross-sectional TEM image (Figure 1B inset) indicates that the nanorods exhibit hexagonal shape. High resolution-TEM (Figure 1C and Figure S1) demonstrates the ordered pore arrays within a single crystalline wall

structure. The plan view along the rod  $c$ -axis (Figure 1C, right) shows the hexagonal arrangement of the micropores; the pore size is measured to be 0.8 nm and the center-to-center distance 1.7 nm. The complementary side-view (Figure 1C, left) indicates that the pore channels run straight across the nanorod length, parallel to the outer surface profile.

The periodicity is measured

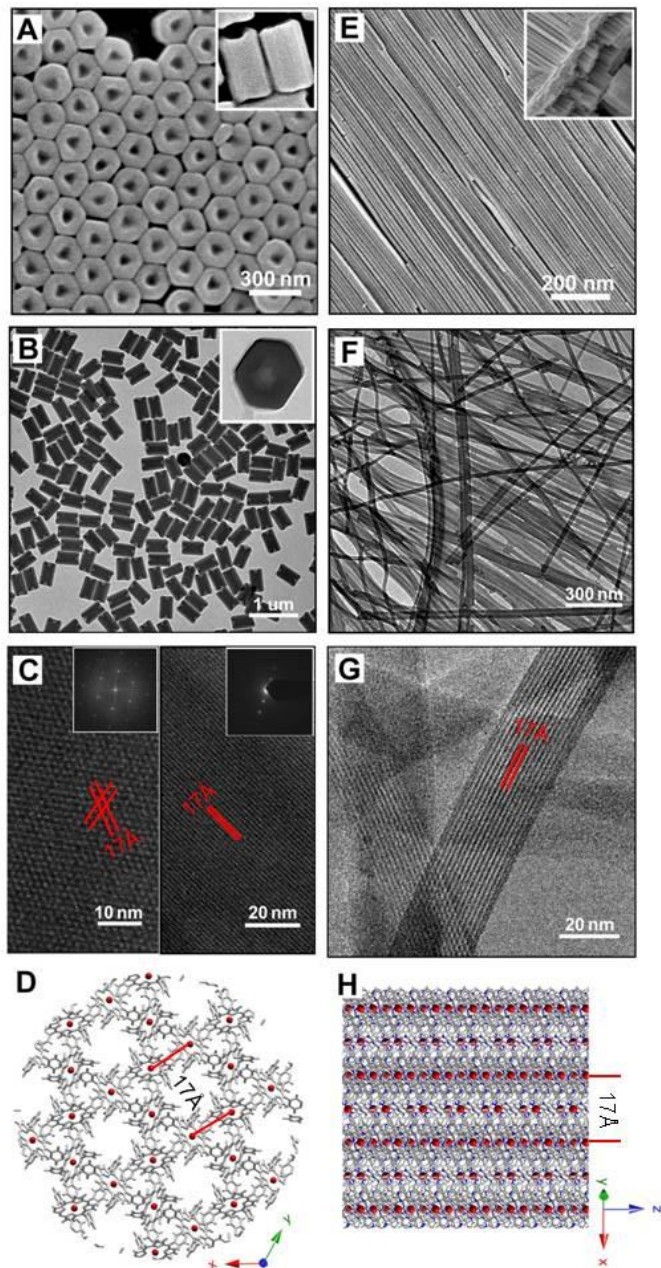


**Figure 1.** Structure of the self-assembled j-aggregate nanostructures. (A) SEM images of monodisperse hexagonal rods prepared using 0.5 mM ZnTPyP (in 0.01 M HCl solution) and 0.01 M Sodium dodecyl sulphate (SDS) at pH 11.3. Inset: cross-sectional SEM image of the nanorods. (B) Corresponding TEM image of the nanorods, inset: end view of a nanorod. (C) HR-TEM of the nanorods, left: side view along the nanorod, inset shows the selected-area electron diffraction (SAED); right: top view of the nanorod, inset shows the FFT. More HR-TEM images are provided in Figure S1. (D) Simulated crystal structure of hexagonal nanorods viewed along the crystallographic  $c$  axis, Zn (red), N (blue), and C (gray). E. SEM image of the nanowires prepared using 0.5 mM ZnTPyP and 0.01 M hexadecyltrimethylammonium bromide (CTAB) at pH 9.5. F. Corresponding TEM image of the nanowires. G. HR-TEM image of the nanowires. H. Simulated crystal structure of the nanowires viewed along the wire.

to be 1.7 nm, consistent with [110] orientation of hexagonal pore structures. Selected-area electron diffraction (SAED) of a single nanorod (Figure 1C left inset) and FFT (Figure 1C right inset) show a single-crystalline pattern. Figure 1F shows a TEM image of the nanowires. The diameter of the nanowires ranges a few nanometers to hundreds of nanometers. Figure 1E shows SEM images for typical nanowires. The length of the nanowires can be controlled from  $\sim 1.5\text{-}\mu\text{m}$  to  $6\text{-}\mu\text{m}$ . TEM imaging shows uniform electron contrast along the nanowires (Figure 1F). High resolution TEM (Figure 1G) indicates an ordered crystalline structure (pore channels) parallel to the nanowire surface profile. The periodicity is measured to be  $\sim 17\text{ \AA}$  suggesting a similar crystal structure to that of the nanorods.

The crystal structures were further characterized by x-ray diffraction (XRD). XRD data show single crystal patterns with major peaks between  $5^\circ$  and  $30^\circ$  (Figure S2). All of the peaks can be indexed as hexagonal space group  $R\bar{3}$  with the unit cell dimensions  $a = b = 33.110\text{ \AA}$ ,  $c = 9.273\text{ \AA}$ ,  $\alpha = \beta = 90^\circ$ , and  $\gamma = 120^\circ$ .<sup>16</sup> Note that the 1D nanostructures exhibit the same XRD patterns despite of their different macroscopic morphologies (nanorod or nanowire), indicating identical crystal structure and unit cell

for the various forms. Figure 1D and H show the crystal structures simulated from the XRD data. In this structural model, each ZnTPyP molecule's central zinc atom is coordinated, in addition to the four pyrrole nitrogens of the same molecule's core, to two pyridyl N-atoms of neighboring ZnTPyPs approaching from both faces. In the framework, each ZnTPyP molecule is bound to four neighbors through four identical Zn-N axial ligations: two at its Zn core and two at opposite ends of its peripheral pyridyl groups, forming hexagonal shape micropores. This leaves two remaining pyridyl groups of ZnTPyP unligated and exposed at pore surfaces.

The adjacent circular hexametric cage arrays interpenetrate each other in the crystal structure through non-covalent  $\pi$ - $\pi$  interactions between macrocyclic monomers, forming pore channels along the *c*-axis, parallel to the wall of the 1D nanostructures. Based on this model, the calculated pore size is 0.92 nm and the periodicity is 1.7 nm, consistent with TEM observations and values calculated from nitrogen isotherms (see Table 1). Such confined 3D cooperative self-assembly through Zn-N axial coordination and non-covalent  $\pi$ - $\pi$  interactions facilitates further growth of the j-aggregate nanostructures, which advantageously allows control over size and aspect ratio of the 1D nanostructures and is not attainable to other methods.<sup>2, 8</sup> Figure 2 shows typical SEM images of the 1D nanostructures with various diameters and lengths. Insight into the j-aggregate growth can be gained from an analysis of the time course of the reaction under the standard conditions monitored by UV-vis spectroscopy and SEM (Figure 3). At the beginning of the reaction (< 4.5 hours), SEM imaging shows no apparent nanostructures were formed. The Soret bands in the corresponding UV-vis spectra of ZnTPyP indicate only aggregated oligomers are formed. After 4.5 hours, well-defined nanocrystals with

hexagonal shape can be observed from SEM imaging. Along with time course, both the diameter and the length of the nanostructures increase with reaction time. The uniformity of the individual nanostructures (size and shape) and surfactants are favorable for formation of ordered assemblies. Formation of extensive j-aggregation is evidenced by apparent red shifts that are likely caused by collective optical behavior from extensive metal-ligand coordination and  $\pi$ - $\pi$  stacking. It is worth noting that the position of the pyridyl groups' nitrogens relative to the macrocyclic ring and the choice of center metal ion are critical to the formation of well-defined morphology. Having the pyridyl nitrogen at the 4-position allows open space to coordinate with central Zn to form stable hexamers that direct further growth with increasing diameters and length. Our experiments indicated that 4-pyridyl monomers and Zn central metal are essential for the formation of 1D nanocrystals. By using 2-pyridyl substituents, 3-pyridyl substituents, or other core metal, we obtained 2D nanosheets and nanospheres instead of 1D nanostructures (See Figure S3).

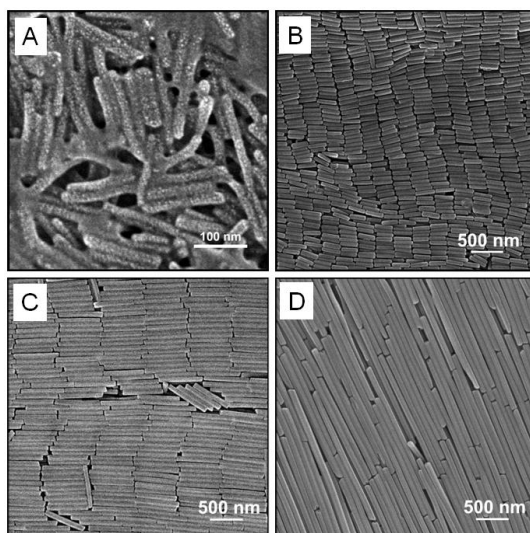


**Figure 2.** Representative SEM images showing controlled size and aspect ratio of 1D nanostructures. (A) diameter ( $d$ ) 15 nm, length ( $l$ ) 120 nm. (B)  $d=35$  nm,  $l=280$  nm. (C)  $d=75$  nm,  $l=800$  nm. (D)  $d=100$  nm,  $l=2.5$   $\mu$ m.

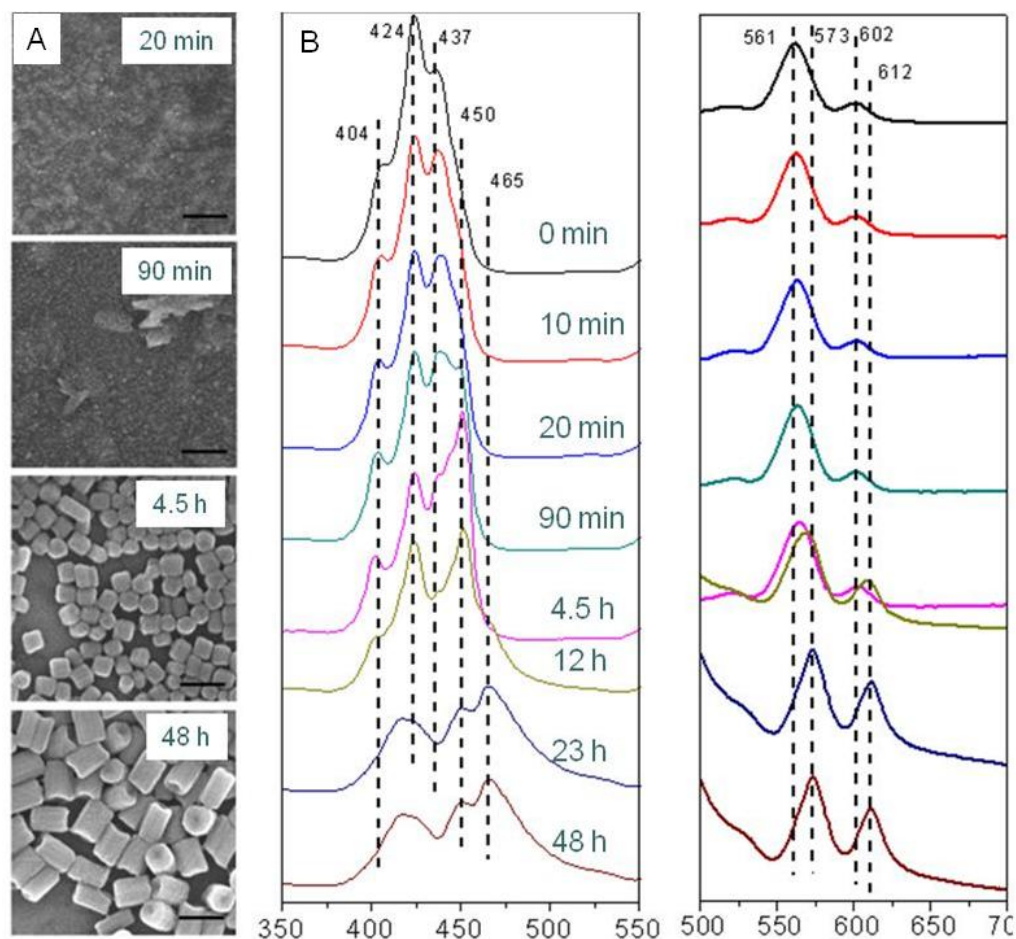


**Figure 3.** Macrocytic monomer aggregation at different reaction times. (A) SEM images and (B) UV-Vis absorption spectra of ZnTPyP nanostructures. In this reaction, 5 ml of stock ZnTPyP solution in water (0.01 M, 0.2 M HCl) was added into 95 ml of SDS 0.01 M solution (0.02 M NaOH) while stirring continuously at room temperature (25 °C) for 48 hours. 0.5 ml samples of the reaction mixture were withdrawn at different times for UV-Vis spectra. The ZnTPyP nanostructures were separated for SEM imaging by centrifugation at 9000 rpm.

Detailed experiments indicated that presence of surfactants with concentration  $C_{surfactant}$  higher than cmc in the self-assembly system is essential. It was discovered that irregular structures were obtained in the absence of surfactants or for  $C_{surfactant}$  lower than cmc (Figure S4). Furthermore, we find that for single-tailed surfactants, an alkane chain of ten or more carbons is required to form well-defined crystalline nanostructures. This is similar to previous observation in which surfactants with longer alkane chains are

necessary for encapsulation of nanoparticles within surfactant micelles because longer alkane chains form more stable micelles to confine nucleation and growth of well-defined nanocrystals.<sup>13</sup> In experiments using ethanol as solvent instead of water, ill-defined nanostructures are obtained. This is probably due to the fact that surfactants do not form micelles in ethanol thus are not able to stabilize or confine the molecular assembly of macrocyclic monomers.

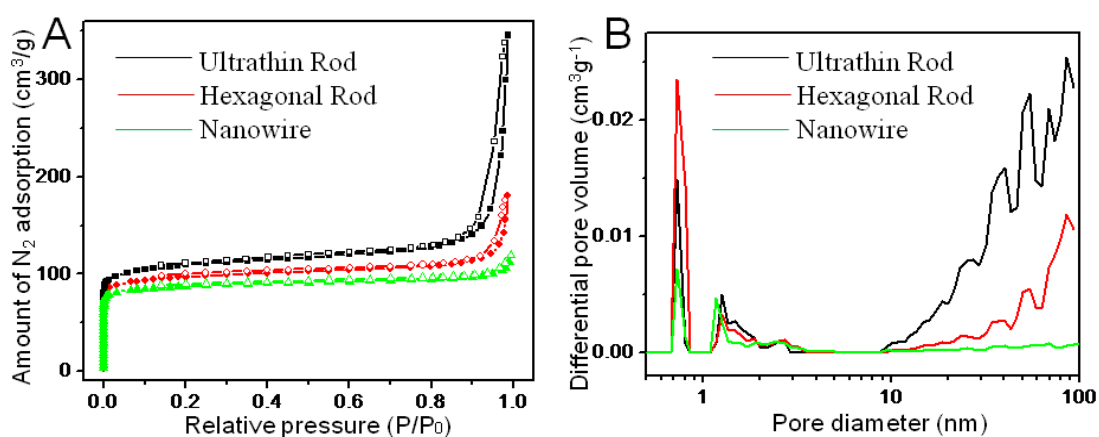


**Figure 4.** Nitrogen isotherms. (A) Nitrogen sorption isotherms obtained at 77 K for different ZnTPyP j-aggregates: ultrathin rods (diameter ~15 nm, length ~70 nm), hexagonal rods (diameter 120 nm, length 500 nm), and nanowires (diameter ~100 nm, length 2.5  $\mu$ m) (adsorption, solid data markers; desorption, open data markers). (B) Micropore size distributions for different ZnTPyP j-aggregates.

**Table 1.** Porosity, surface area, and pore size of different ZnTPyP nanostructures.

	Porosity (%)	Surface area (m <sup>2</sup> /g)	Pore size (Å)
Thin nanorods	34.3	371	8.1
Hexagonal nanorods	20.1	327	7.9
Nanowires	16.1	294	7.8

Nitrogen sorption isotherms were performed to characterize the pore structures of the 1D nanostructures. Nitrogen adsorption/desorption isotherms and corresponding micropore size distributions for different ZnTPyP j-aggregates are shown in Figure 4, and the calculated porosity, surface area, and average micropore size are summarized in Table 1. The nitrogen isotherms are characteristic of type I isotherms without apparent hysteresis. BET measurement shows a maximum surface area of 371 m<sup>2</sup>/g for the nanorod structure. The pore size distribution shows a major peak at ~ 0.8 nm that corresponds to the hexagonal crystal lattice of self-assembled nanocrystals (Figure 1C). The porosity of these j-aggregates is maintained after degassing at 50°C for 48 hours suggesting stability of the pore structure. In addition to the micropore, there also exist mesopores and macropores ranging from 2 to 100 nm (Figure 3B) that is probably due to the packing of nanorods and nanowires. Our thermogravimetric analysis (TGA) results show these aggregates are thermally stable up to ~450 °C (Figure S5) before they are carbonized. In addition to physical sorption, we have discovered that these j-aggregate nanostructures show a specific chemical sorption of NO. The nanorods show ~4wt% NO absorption at 1 atm and ~34wt% NO absorption at 10 atm (Figure S6). We performed TGA on the specimens after exposure to NO to further confirm NO absorption. The results show a consistent weight loss at about ~190°C. Fourier transform infrared spectroscopy results suggest that NO coordinates to central Zn ions (Figure S7).<sup>17</sup>

The j-aggregate nanostructures exhibit properties resulting from individual monomers and their ordered assemblies. They generally retain the optical properties of individual macrocyclic monomers while exhibiting collective optical behavior. Absorption spectra of self-assembled j-aggregates show more complicated signals in

comparison to those of molecular ZnTPyP (Figure S8). The fluorescence image of the 1D nanowires is shown in Figure S9B. Aggregation of ZnTPyP results in new fluorescent signals. Photoluminescence measurements of the nanorods reveal two extra emissions centered at 510-nm and 650-nm in comparison with molecular ZnTPyP (Figure S9A). This may be due to the self-assembly of macrocyclic monomer and the  $\pi$ - $\pi$  interactions of conjugated macrocyclic rings.

### 3. Conclusion

In summary, we have developed a facile confined cooperative self-assembly process to synthesize 1D j-aggregate nanostructures. Through surfactant-assisted non-covalent interactions, nanorods and nanowires with controlled dimension and morphology can be prepared. The 1D nanostructures exhibit unique optical and electrical properties, enhanced over properties of individual monomers due to collective behavior resulting from their assembly. Through kinetic control, our method readily allows for fine-tuning of nanostructure, dimension, and function on multiple length scales. At the molecular level, ZnTPyPs with well-defined size and chemistry possess unique optical and photo-catalytic properties for synthesis of metallic structures. On the nanoscale, controlled assembly of macrocyclic monomers leads formation of ordered nanostructures with precisely defined size, shape, and spatial monomer arrangement so as to facilitate intermolecular mass and energy transfer or delocalization. The capability of exerting rational control over dimension and morphology provides new opportunities for applications in sensing,<sup>20</sup> nanoelectronics,<sup>21</sup> and optics.<sup>22, 23</sup>

## 4. References

1. Zang, L.; Che, Y.; Moore, J. S. *Acc. Chem. Res.* **2008**, 41, (12), 1596-1608.
2. Wang, Z.; Medforth, C. J.; Shelnut, J. A. *J. Am. Chem. Soc.* **2004**, 126, (49), 15954-15955.
3. Stupp, S. I.; LeBonheur, V.; Walker, K.; Li, L. S.; Huggins, K. E.; Keser, M.; Amstutz, A. *Science* **1997**, 276, (5311), 384-389.
4. Li, F.; He, J.; Zhou, W. L.; Wiley, J. B. *J. Am. Chem. Soc.* **2003**, 125, (52), 16166-16167.
5. Gan, H.; Liu, H.; Li, Y.; Liu, Y.; Lu, F.; Jiu, T.; Zhu, D. *Chem. Phys. Lett.* **2004**, 399, (1-3), 130-134.
6. Wang, P.-p.; Bai, B.; Hu, S.; Zhuang, J.; Wang, X. *J. Am. Chem. Soc.* **2009**, 131, (46), 16953-16960.
7. Wang, Z.; Medforth, C. J.; Shelnut, J. A. *J. Am. Chem. Soc.* **2004**, 126, (51), 16720-16721.
8. Hu, J.-S.; Guo; Liang, H.-P.; Wan, L.-J.; Jiang, L. *J. Am. Chem. Soc.* **2005**, 127, (48), 17090-17095.
9. Tsuruoka, T.; Furukawa, S.; Takashima, Y.; Yoshida, K.; Isoda, S.; Kitagawa, S. *Angew. Chem. Int. Ed.* **2009**, 48, (26), 4739-4743.
10. Mauzerall, D. C. *Clinics in Dermatology* **1998**, 16, (2), 195-201.
11. Drain, C. M.; Varotto, A.; Radivojevic, I. *Chem. Rev.* **2009**, 109, (5), 1630-1658.
12. Blankenship, R. E., *Molecular Mechanisms of Photosynthesis*. Blackwell, Oxford: 2002.

13. Fan, H.; Yang, K.; Boye, D. M.; Sigmon, T.; Malloy, K. J.; Xu, H.; Lopez, G. P.; Brinker, C. J. *Science* **2004**, 304, (5670), 567-571.
14. Bai, F.; Wu, H.; Haddad, R. E.; Sun, Z.; Schmitt, S. K.; Skocypec, V. R.; Fan, H. *Chem. Commun.* 46, (27), 4941-4943.
15. Barber, D. C.; Freitag-Beeston, R. A.; Whitten, D. G. *J. Phys. Chem.* **2002**, 95, (10), 4074-4086.
16. Krupitsky, H.; Stein, Z.; Goldberg, I.; Strouse, C. E. *J. Inclusion Phenom.* **1994**, 18, 177.
17. Israelachvili, J. N.; Mitchell, D. J.; Ninham, B. W., 1525–1568. *J. Chem. Soc.* **1976**, 2, 1525–1568.
18. Song, Y.; Garcia, R. M.; Dorin, R. M.; Wang, H.; Qiu, Y.; Shelnut, J. A. *Angew. Chem. Int. Ed.* **2006**, 45, (48), 8126-8130.
19. Song, Y.; Yang, Y.; Medforth, C. J.; Pereira, E.; Singh, A. K.; Xu, H.; Jiang, Y.; Brinker, C. J.; van Swol, F.; Shelnut, J. A. *J. Am. Chem. Soc.* **2003**, 126, (2), 635-645.
20. Rakow, N. A.; Suslick, K. S. *Nature* **2000**, 406, ( ), 710-713.
21. Schwab, A. D.; Smith, D. E.; Bond-Watts, B.; Johnston, D. E.; Hone, J.; Johnson, A. T.; de Paula, J. C.; Smith, W. F. *Nano Letters* **2004**, 4, (7), 1261-1265.
22. Winkelmann, C. B.; Ionica, I.; Chevalier, X.; Royal, G.; Bucher, C.; Bouchiat, V. *Nano Letters* **2007**, 7, (6), 1454-1458.
23. Medforth, C. J.; Wang, Z.; Martin, K. E.; Song, Y.; Jacobsen, J. L.; Shelnut, J. A. *Chem. Commun.* **2009**, DOI: 10.1039/b914432c, -.

## 5. Appendix: Supporting Figures and Materials

### 1. Materials:

All the macrocyclic monomers were purchased from Frontier Scientific and used without further purification. All the surfactants were purchased from Aldrich and used without further purification.

**2. 1D j-aggregate nanostructure synthesis:** Typically, 0.5 ml of ZnTPyP solution (0.01 M, 0.2 M HCl) was added into 9.5 ml of surfactant solution (such as SDS, CTAB etc. 0.01 mM, containing 0.02 mM NaOH) with continuous stirring, and the mixture was stirred at room temperature (25 °C) for 48 hours. The procedures for the other experiments were similar to that for the typical one, but altering either surfactant type and concentration, or NaOH concentration (resulting in different pH values after mixing), or ratios of porphyrin to surfactants. We can control the morphology and size of these ZnTPyP j-aggregates by adjustment of above experiment parameters.

**3. Photocatalytic reaction:** In a typical metallization of ZnTPyP nanowires, 10 ml of the colloidal suspension of ZnTPyP nanowire (prepared by the same synthesis described above) was placed in a 20-ml scintillation glass vial. The  $K_2PtCl_4$  stock solution 0.5 ml (10 mM Pt) and ascorbic acid stock solution 0.5 ml (0.1 M) were added under stirring. The vial was shaken in an ultrasound bath, and irradiated with incandescent light (800 nmol irradiation) from a projector lamp (360 W) for 30 min. The solution became black solution after irradiation. The black solution was centrifuged at 3000 rpm and washed twice with Millipore water. We can get Pt/ZnTPyP nanowires with different Pt thickness by tuning Pt concentration in the reaction.

**4. Adsorption of nitric oxide (NO):** it was studied using a Tapered-Element Oscillating Microbalance Pulse Mass Analyzer (TEOM-PMA) from Rupprecht and Patashnick (Albany, NY). Approximately 50mg sample was loaded into the TEOM, and was purged with nitrogen at 30 °C and atmospheric pressure overnight. Adsorption of NO (x% in nitrogen) was carried out at 30 °C and at either ambient pressure or 10 atm under dynamic flow conditions; ~ 20 sccm. The mass of the sample was monitored continuously during NO adsorption. In order to check for physisorbed NO, the NO feed was periodically replaced with nitrogen which was demonstrated separately not to adsorb onto the sample at either 1 or 10 atm. The stability of the measured sample mass during nitrogen flow indicated that NO was not merely physisorbed onto the sample, but was chemisorbed.

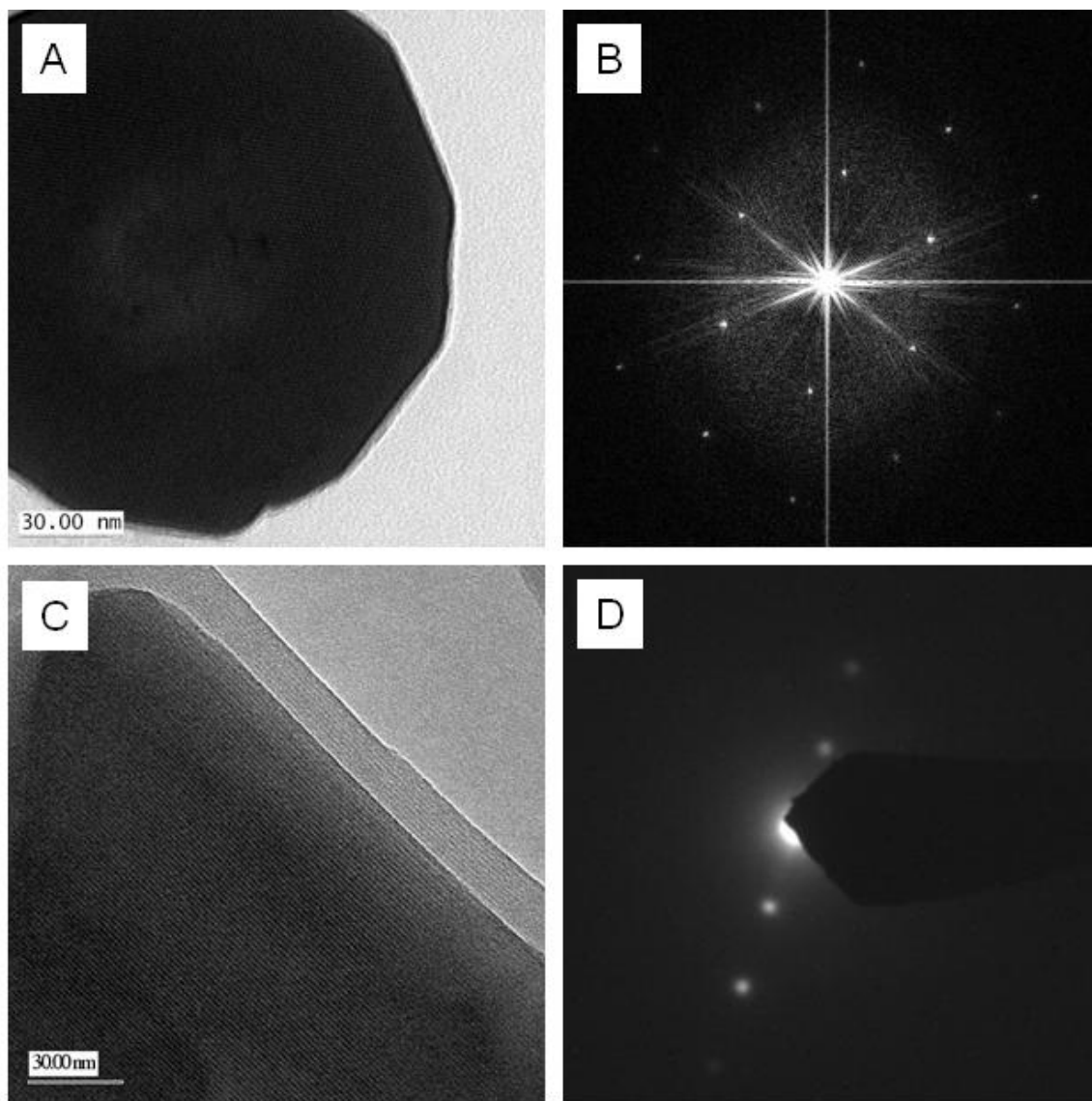


Figure S1. HR-TEM of the nanorods, A: end view of the nanorod, B: FFT image of A; C: side view of the nanorod; D: selected-area electron diffraction (SAED) of C

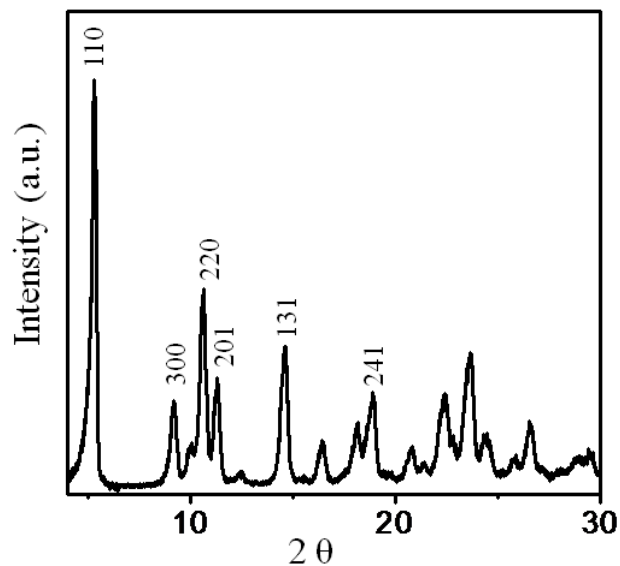


Figure S2. XRD powder pattern of ZnTPyP nanorods.

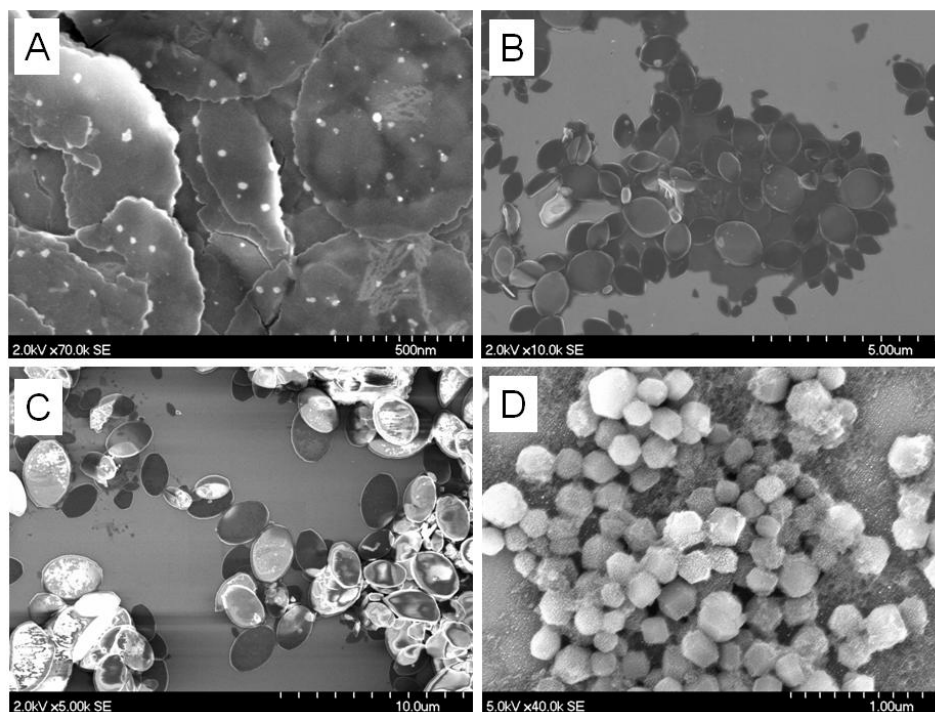


Figure S3. SEM images of self-assembled nanomaterials produced using different porphyrin substituents and core metals.

- A. CTAB 0.01 M, Zn(II) meso-Tetra (2-Pyridyl) Porphyrin 0.5 mM, pH 11.45
- B. CTAB 0.01 M, Zn(II) meso-Tetra (3-Pyridyl) Porphyrin 0.5 mM, pH 11.37
- C. SDS 0.01 M, Zn (II) meso-Tetra (2-Pyridyl) Porphyrin 0.5 mM, pH 11.32
- D. CTAB 0.01 M, Co(III) meso-Tetra (4-Pyridyl) Porphyrin 0.5 mM, pH 11.12

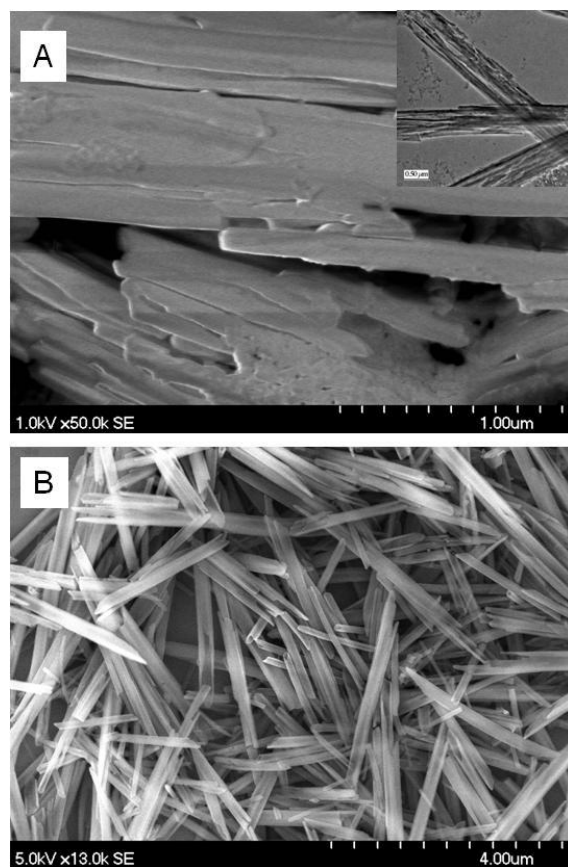


Figure S4. SEM image of irregularly shaped ZnTPyP structures synthesized without using surfactants (A) and with surfactant SDS concentration lower than cmc (2.5 mM), confirm the SDS cmc The CMC of SDS in pure water at 25°C is 8.2mM. (B).

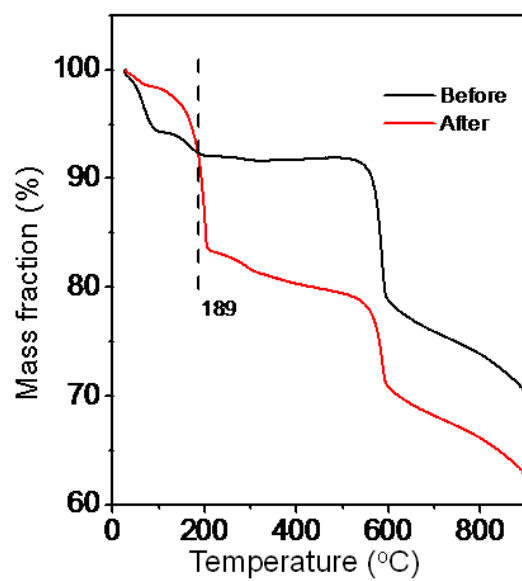


Figure S5. TGA results for ZnTPyP nanostructures before and after NO absorption.

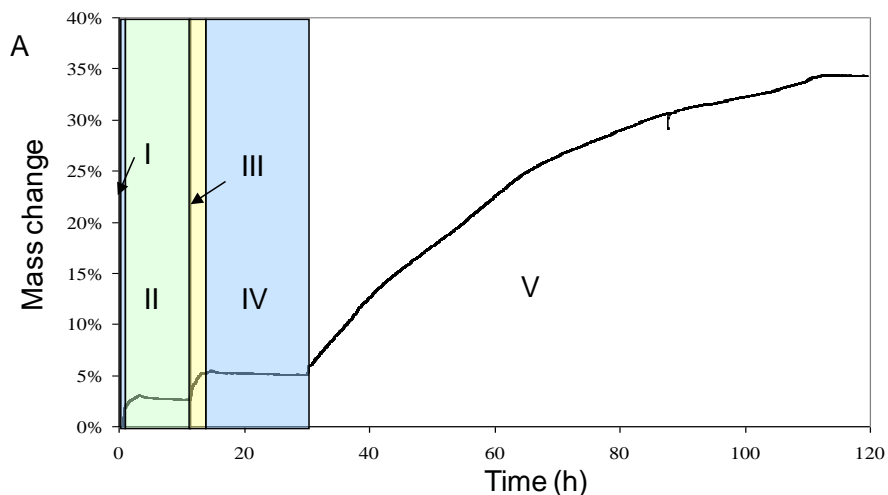


Figure S6. Chemical absorption of NO onto ZnTPyP nanorods.

- I. Baseline ( $N_2$  at 1 atm).
- II. NO chemical absorption at 1 atm.
- III. NO chemical absorption at 10 atm.
- IV.  $N_2$  purge at 10 atm.
- V. NO chemical absorption at 10 atm (resumed).

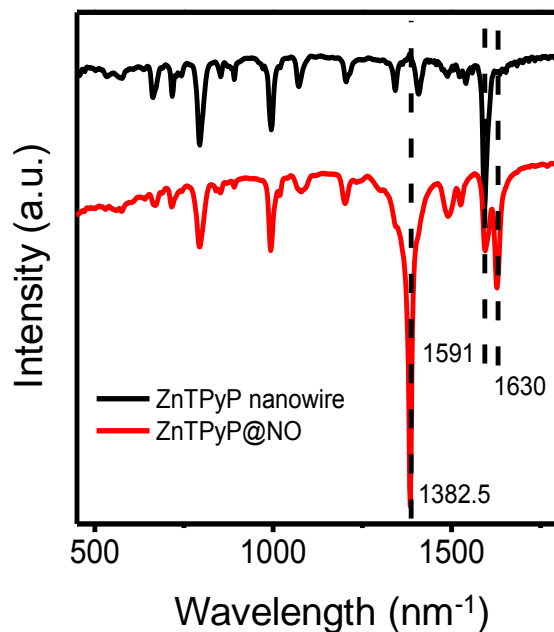


Figure S7. FTIR spectra of ZnTPyP nanowire before and after NO chemical absorption.

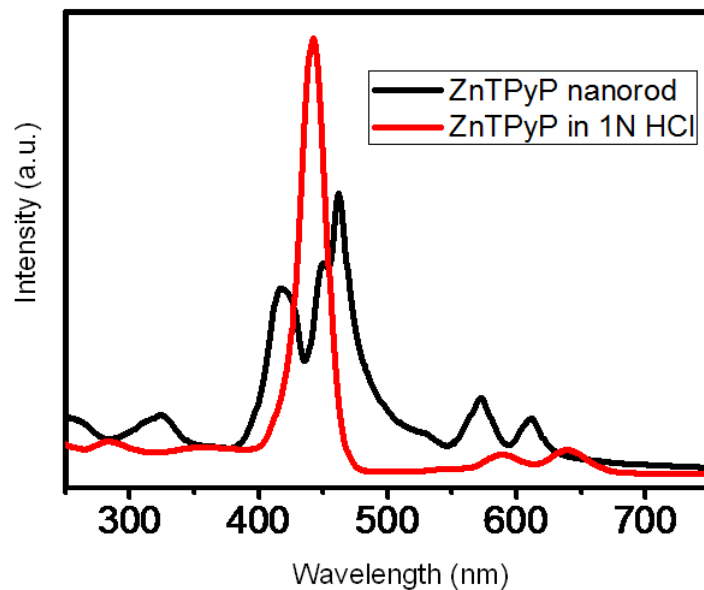


Figure S8. UV-Vis of ZnTPyP in 1N HCl and ZnTPyP nanorod dispersed in water

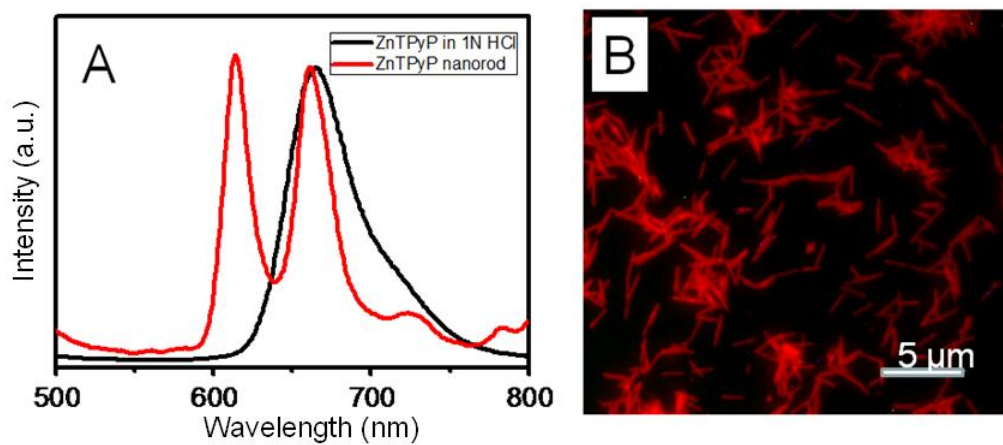


Figure S9. A. Fluorescence spectra of ZnTPyP in 1N HCl and ZnTPyP nanorods dispersed in water; B. Fluorescence image of ZnTPyP nanowires.

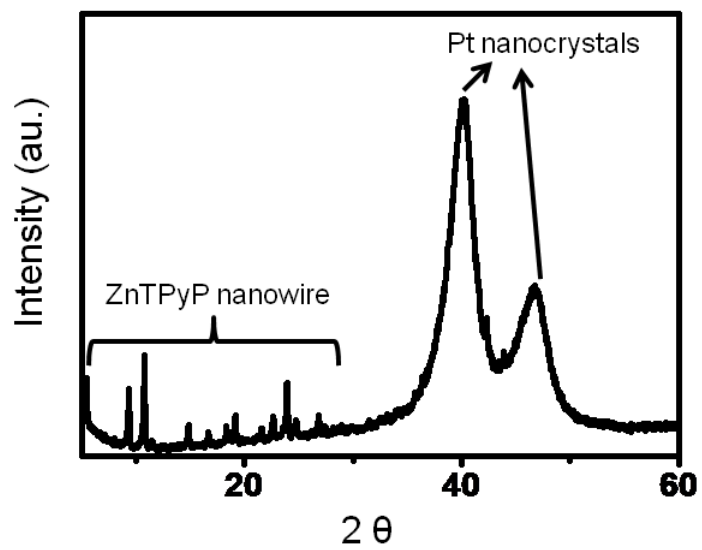


Figure S10. XRD powder pattern of Pt/ZnTPyP nanocomposite materials.

## 6. Distribution

1	MS 1349	Hongyou Fan, 1815
1	MS 1349	William Hammetter, 1815
1	MS 1349	Eric Coker, 1815
1	MS 1411	Mark Rodriguez, 1822
1	MS 1303	Jianyu Huang, 1132
1	MS 0359	Donna Chavez, 1911
1	MS 0899	Technical Library, 9536 (electronic copy)

